

Experimental observation of attenuated-total-reflection spectra of a GaAs/AlAs superlattice

M. Haraguchi and M. Fukui

*Department of Electrical and Electronic Engineering, Faculty of Engineering,
The University of Tokushima, Tokushima 770 Japan*

S. Muto

Fujitsu Laboratories Limited, Atsugi City, Kanagawa 243-01 Japan

(Received 7 September 1989)

We present the first experimental observation of the attenuated-total-reflection (ATR) spectra of a GaAs/AlAs superlattice. The ATR spectra clearly show the excitation of surface-phonon polaritons on the semiconductor superlattice. We have, moreover, evaluated the dielectric parameters of GaAs and AlAs through a theoretical ATR-spectra fit to the experimental ones. These parameters are compared with those reported previously.

Recently, there has been considerable interest in the physical properties of semiconductor superlattices (SL's) and multiple quantum wells (MQW's), from the viewpoint of the applications for optoelectronic or high-speed devices. Although there have been a number of reports on the electronic properties of these structures, only a few studies of the optical properties, particularly in the infrared and far infrared, have been carried out.¹⁻³ Information about the optical properties of SL's in such a frequency region is thus not enough. For instance, there are no accurate dielectric parameters for an AlAs film with thickness below 10 nm, which is widely employed as a part of the SL's, in the infrared and far infrared when we wish to describe the dielectric constant by the classical-oscillator model.

In measuring optical properties of materials, attenuated-total-reflection (ATR) spectroscopy is known to be a powerful and versatile technique.^{4,5} In particular, the ATR method has proven to be a more sensitive probe for the measurement of the optical constants of thin layers than direct optical-reflection methods without any prism. That is because the ATR technique leads to the excitation of surface polaritons (SP's), whose characteristics are quite sensitive to the optical properties of thin layers.

Some groups⁶⁻¹⁰ have already shown theoretical ATR spectra of SL's. El-Gohari *et al.*¹¹ have successfully observed the ATR spectra of a GaAs/Al_xGa_{1-x}As MQW sample. In their sample, the thickness of the Al_{0.35}Ga_{0.65}As barrier is so thick (17 nm) that electron and hole states of each GaAs well cannot be coupled to those of neighbor wells, i.e., it is a MQW sample. However, to our knowledge, for SL samples in which electron and hole states of wells can overlap each other, no experimental observations of ATR spectra for semiconductor SL's have been reported yet.

In this paper, we present experimental observation of ATR spectra of a GaAs/AlAs SL sample grown by molecular-beam epitaxy (MBE) in the frequency range of 250–600 cm⁻¹. Consequently, it is found that the ATR spectrum contains a resonance due to the excitation of SP's on the GaAs/AlAs SL. Finally, we have determined

optical constants of GaAs and AlAs through a theoretical fit to the experimental ATR data. The SP's are electromagnetic waves that travel along an interface consisting of two media where one of them (surface-wave active) has a negative real part of the dielectric constant and the other (surface-wave inactive) has a positive one in appropriate spectral ranges.^{4,5} Since the SP's on SL's are generated by linear superpositions of SP's localized in the vicinity of the respective interfaces between two layers,⁷ the SL's should be composed of a surface-wave active material and a surface-wave inactive material.

We¹⁰ have already theoretically shown that the SP's on semi-infinite and finite GaAs/Al_{0.3}Ga_{0.7}As SL's exist. Along the line of a previous procedure,^{8,10} the theoretical ATR spectra of a GaAs/AlAs SL are calculated and adjusted to experimental spectra to obtain optical constants of GaAs and AlAs and thicknesses of respective layers.

We assume the optical constants of respective layers to be described by the oscillator model as

$$\epsilon(\omega) = \epsilon_{\infty} + \frac{S\omega_{TO}^2}{\omega_{TO}^2 - \omega^2 - i\nu\omega}, \quad (1)$$

where ω is the angular frequency, ϵ_{∞} the high-frequency dielectric constant, S the oscillator strength, ω_{TO} the angular frequency of the transverse-optical phonon, and ν the collision frequency of the transverse-optical phonon.

Using respective optical parameters of GaAs (Ref. 12) and AlAs (Ref. 13), as listed in Table I, we evaluated the frequency dispersions of the optical constants of GaAs and AlAs from Eq. (1), as displayed in Fig. 1. Note that we adopted the optical constants of the AlAs film of 1.2- μ m thickness. It is found that GaAs is surface-wave active in the frequency region 269–293 cm⁻¹, while AlAs is inactive there. This suggests that the SP's should be produced on the GaAs/AlAs SL's in the frequency range 269–293 cm⁻¹. Similarly, the SP's should also be produced in the frequency range 362–404 cm⁻¹. AlAs is then surface-wave active and GaAs is inactive. Namely, it is predicted that ATR dips could be observed in two frequency regions.

TABLE I. The dielectric parameters of GaAs and AlAs. The upper values were cited from Refs. 7 and 8 and the lower values have been obtained by the present work.

| | ϵ_∞ | ω_{TO} (cm^{-1}) | S | ν (cm^{-1}) |
|-------------|-------------------|---|------|----------------------------|
| GaAs | | | | |
| Reference 7 | 10.9 | 269.2 | 2.03 | 2.5 |
| This work | 11.0 | 264.5 | 2.13 | 3.9 |
| AlAs | | | | |
| Reference 8 | 8.2 | 361.8 | 1.9 | 8.0 |
| This work | 8.5 | 361.2 | 1.87 | 4.2 |

On calculating ATR curves, we have to take into account a wavelength dispersion of the optical constant of a KRS-5 prism adopted here. It is written as¹⁴

$$\epsilon_p(\lambda_0) = 1 + \sum_{i=1}^5 \frac{a_i \lambda_0^2}{\lambda_0^2 - \lambda_i^2}, \quad (2)$$

where $a_1 = 1.8293958$, $a_2 = 1.6675593$, $a_3 = 1.1210424$, $a_4 = 0.0451336$, $a_5 = 12.380234$, $\lambda_1^2 = 0.0225$, $\lambda_2^2 = 0.0625$, $\lambda_3^2 = 0.1225$, $\lambda_4^2 = 0.2025$, $\lambda_5^2 = 27089.737$, and λ_0 is the wavelength in μm .

The sample, which was fabricated at the Fujitsu Laboratories Ltd., is the GaAs/AlAs superlattice grown on an undoped semi-insulating GaAs substrate by the MBE method. The SL consists of alternate 5.0-nm-GaAs well layers and 5.0-nm-AlAs barrier layers of total thickness 500 nm, and GaAs buffer-layer thickness is 300 nm. This sample was not doped intentionally.

The frequency-scan ATR spectra were obtained utilizing the ATR apparatus with a KRS-5 half-cylinder prism set up in a Hitachi 270-50 optical spectrometer (250–4000 cm^{-1}) at room temperature. We employed the Otto ATR configuration.¹⁵ The sample ($18 \times 9 \text{ mm}^2$) was pressed against the prism through a 3- μm -thick spacer with a window of $15 \times 7 \text{ mm}^2$ in cross section. A collimated and *p*-polarized infrared radiation from a globar was incident upon the prism. The angle of incidence was fixed

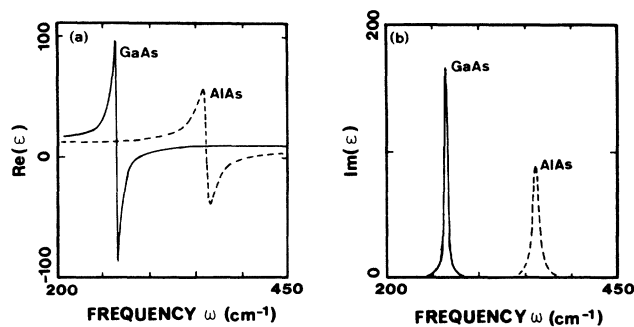


FIG. 1. The frequency dispersion of the dielectric constants of GaAs and AlAs, calculated by the parameters presented in Refs. 7 and 8. The solid and dashed lines correspond to the dielectric constants of GaAs and AlAs, respectively. (a) The dispersion of a real part of the dielectric constants, $\text{Re}(\epsilon)$. (b) The dispersion of an imaginary part of the dielectric constants, $\text{Im}(\epsilon)$.

at 35° and the frequency range was varied from 250 to 600 cm^{-1} , with a resolution of 2 cm^{-1} .

Figure 2 shows an experimental ATR curve (solid line). There are two structures around 280 and 380 cm^{-1} in the ATR spectrum, i.e., an intensely sharp dip at 280 cm^{-1} and a broad dip at 380 cm^{-1} . The structure around 380 cm^{-1} consists of two dips, i.e., at 373 and 397 cm^{-1} . This structure is not due to inhomogeneity of the sample structure, e.g., thickness irregularity of well and/or barrier, or thickness inhomogeneity of the air gap between the prism and the sample, and so on. It will be confirmed later that the structures around 280 and 380 cm^{-1} come from the excitation of surface-phonon polaritons on the SL's. Since the transmittance of the KRS-5 prism is quite low below 265 cm^{-1} , the experimental spectrum is not accurate in its frequency region.

Next we calculate a theoretical ATR curve by making a least-squares fit to the experimental ATR curve to determine the dielectric parameters of GaAs and AlAs. The theoretical curve can be adjusted to the experimental one using nine variable quantities which are the dielectric parameters, i.e., ϵ_∞ , S , ω_{TO} , and ν , of GaAs and AlAs and the thickness of the air gap.

The fitted curve is shown by the dashed line in Fig. 2. The agreement between the two is primarily good, except below 265 cm^{-1} . The large deviation between the two spectra in the frequency around 260 cm^{-1} is produced by low transmittance of the KRS-5 prism, as mentioned already. Comparing the two spectra in detail, the calculated result successfully reproduces the dip at 280 cm^{-1} and the broad dip around 380 cm^{-1} . However, unfortunately, there are small discrepancies, i.e., the depth of the dip at 280 cm^{-1} and an oscillatory fashion between 375 and 390 cm^{-1} which is more clearly confirmed in the magnified part in Fig. 2. The discrepancy for the latter may be due to zone-folding LO phonons of GaAs and AlAs in the SL (Ref. 16) or the frequency dependence of the collision frequencies of TO phonons in GaAs and AlAs, which we did not take into account in our calculation. The discrepancy

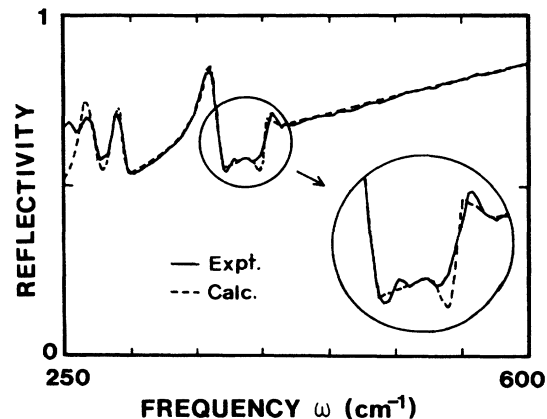


FIG. 2. The experimental (solid line) and theoretical (dashed line) frequency-scan (250–600 cm^{-1}) ATR spectra of the GaAs/AlAs [(5.0 nm/(5.0 nm), 50 period] superlattice in the Otto ATR configuration. The thickness of the air gap is 3 μm and the angle of incidence is 35° .

for the former probably arises from the low transmittance of the KRS-5 prism.

In Table I, we present the dielectric parameters of GaAs and AlAs estimated by the fitting technique mentioned above. Comparing the dielectric parameters evaluated by the present work with those obtained by Kim and Spitzer¹² and Perkowitz, Sudharanan, and Yom,¹³ the phonon frequency for GaAs is shifted to a lower-frequency side and the damping factor for AlAs is much smaller. This frequency shift may be caused by a stress in the GaAs and AlAs layers. Namely, in the GaAs and AlAs SL's, there is a tensile stress in the GaAs layers and a compressive stress in the AlAs layers because of lattice mismatch between GaAs and AlAs and discrepancy of thermal expansion coefficients.¹⁷ The tensile stress in GaAs makes the phonon frequency of GaAs shift to a lower side and the compressive stress in AlAs layers makes that of AlAs shift to a higher side. On the contrary, the result shows that the phonon frequency of AlAs, as well as that for GaAs, shifts slightly to a lower side. Hence the phonon frequency shift of GaAs to the lower side cannot be explained only by the stress.

Anharmonicities of phonons¹⁸ of GaAs and AlAs are probably other candidates leading to the frequency shift. Including the anharmonic effect, the frequency of phonon shifts to a lower side and the damping factor shows the large frequency dependence. The result that the phonon frequency in AlAs shifts to the lower side indicates that the anharmonic effect is not negligible. In our sample, the thickness of GaAs and AlAs layers is only 5.0 nm, and hence each layer cannot be released from the stress. Consequently, the anharmonicity in each layer will probably become significant. On the other hand, since Kim and Spitzer adopted the GaAs layer with a layer thickness of 200 μm and Perkowitz, Sudharanan, and Yom employed an AlAs layer of 1.2- μm thickness, GaAs and AlAs layers could be released from the stress and the strain and physical properties of their materials may be basically the same as those of the "bulk" ones.

The major discrepancy between their data and ours is on the collision frequency of the TO phonon in the AlAs layers. This is most likely attributable to quality of sample, especially AlAs layers. The quality may be discussed through information about the amount of impurities and carrier concentrations, uniformity of the thickness of the well and barrier layers, and smoothness of interfaces consisting of GaAs and AlAs. The carrier concentration of our sample is about $10^{14}/\text{cm}^3$, being on the lowest level for samples fabricated by the current MBE technology. The uniformity of each layer thickness and smoothness of interfaces are very good. From the above statements, the quality of our sample must be excellent, leading to the small collision frequency of the TO phonon in AlAs layers.

To discuss the origin of the dips in Fig. 2, we calculate the depth profiles of the electric field intensity $|E_x|$ parallel to the sample surface by using the optical parameters obtained by the present work, as shown in Fig. 3.

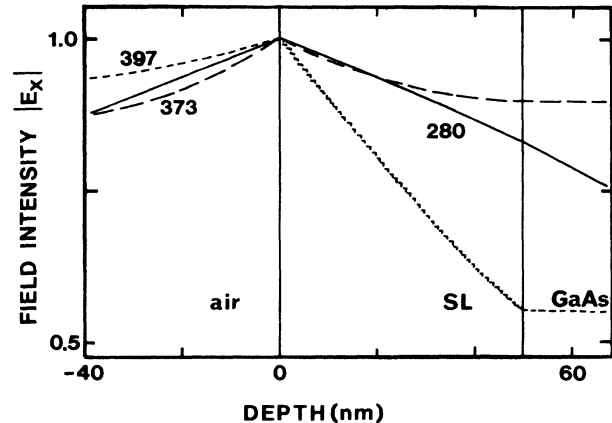


FIG. 3. The x component of the electric field $|E_x|$ at 280, 373, and 397 cm^{-1} (at resonance frequencies in Fig. 2). The value of E_x is normalized by one at the air-gap-SL interface. The x direction is along the interface.

Note that $|E_x|$ at the sample surface is set to unity. The field intensity at 280 cm^{-1} (solid line) is localized at the SL surface and decays into the substrate, associated with the intense resonance. On the other hand, $|E_x|$ at 373 (long-dashed line) and 397 cm^{-1} (short-dashed line) are localized at the air-SL interface and do not decay in the substrate. At 280 and 373 cm^{-1} $|E_x|$ peaks at the SL surface and exponentially decays away from it in the SL layer. Moreover, a real part of λ in Eq. (13) in Ref. 5, which is the indication of whether the mode is SP or not, is larger than an imaginary one. These reflect the character of SP's mode, so the dips at 280 and 373 cm^{-1} are recognized as being due to the excitation of SP's on the GaAs/AlAs SL.

$|E_x|$ at 397 cm^{-1} is also bound at the SL surface. However, $\text{Re}(\epsilon_{\text{AlAs}}) < 0$, $|\text{Re}(\epsilon_{\text{AlAs}})| \approx |\text{Im}(\epsilon_{\text{AlAs}})|$, and $|\text{Re}(\epsilon_{\text{AlAs}})| < |\text{Re}(\epsilon_{\text{GaAs}})|$, where $\text{Re}(x)$ and $\text{Im}(x)$ means the real part of x and the imaginary part of x , respectively. This mode is very lossy, and is therefore not a so-called Fano mode.¹⁹ Figure 3 shows that distribution of $|E_x|$ is steplike in the SL, where E_x does not vary in the GaAs layer but does in the AlAs layer.

As is well known, two types of surface modes exist on films of finite thickness.^{4,5} The dip at 397 cm^{-1} is due to the excitation of the high-frequency branch of the SP in the AlAs layers. On the other hand, the dip at 373 cm^{-1} is due to the excitation of the low-frequency branch.

We have presented the experimental ATR spectra of the GaAs/AlAs superlattice in the Otto geometry and attributed the structures at around 280 and 380 cm^{-1} to the excitation of surface-phonon polaritons in the SL as predicted by theory. Moreover, the dielectric parameters of GaAs and AlAs have been determined by fitting theoretical ATR spectrum to experimental one. We have pointed out the collision frequency of the TO phonon in the AlAs layer employed here is much smaller than that obtained previously.

- ¹A. K. Sood, J. Menendez, M. Cardona, and K. Ploog, *Phys. Rev. Lett.* **54**, 2115 (1985).
- ²K. A. Maslin, T. J. Parker, N. Raj, D. R. Tilley, P. J. Dobson, D. Hilton, and C. T. B. Foxon, *Solid State Commun.* **60**, 461 (1986).
- ³B. C. Covington, C. C. Lee, B. H. Hu, H. F. Taylor, and D. C. Streit, *Appl. Phys. Lett.* **54**, 2145 (1989).
- ⁴*Surface Polaritons*, edited by V. M. Agranovich and A. A. Maradudin (North-Holland, Amsterdam, 1982).
- ⁵*Electromagnetic Surface Modes*, edited by A. D. Boardman (Wiley, New York, 1982).
- ⁶R. E. Camley and D. L. Mills, *Phys. Rev. B* **29**, 1695 (1984).
- ⁷B. L. Johnson, J. T. Weiler, and R. E. Camley, *Phys. Rev. B* **32**, 6544 (1985).
- ⁸M. Fukui and K. Matsugi, *J. Phys. Soc. Jpn.* **56**, 2964 (1987).
- ⁹N. Raj, R. E. Camley, and D. R. Tilley, *J. Phys. C* **20**, 5203 (1987).
- ¹⁰Y. Nagano, K. Matsugi, M. Haraguchi, and M. Fukui, *J. Phys. Soc. Jpn.* **58**, 733 (1989).
- ¹¹A. R. El-Gohari, T. J. Parker, N. Raj, D. R. Tilley, P. J. Dobson, D. Hilton, and C. T. R. Foxon, *Semicond. Sci. Technol.* **4**, 338 (1989).
- ¹²O. K. Kim and W. G. Spitzer, *J. Appl. Phys.* **50**, 4362 (1979).
- ¹³S. Perkowitz, R. Sudharanan, and S. S. Yom, *Solid State Commun.* **62**, 645 (1987).
- ¹⁴W. S. Rodney and I. H. Malitson, *J. Opt. Soc. Am.* **46**, 956 (1956).
- ¹⁵A. Otto, *Z. Phys.* **216**, 398 (1968).
- ¹⁶M. Nakayama, K. Kubota, T. Kanata, H. Kato, S. Chika, and N. Sano, *Jpn. J. Appl. Phys.* **24**, 1331 (1985).
- ¹⁷T. Nishioka, Y. Shinoda, and Y. Ohmachi, *J. Appl. Phys.* **57**, 277 (1985).
- ¹⁸K. Hisano, F. Placido, A. D. Bruce, and G. D. Holah, *J. Phys. C* **5**, 2511 (1972).
- ¹⁹P. Halevi, *Surf. Sci.* **76**, 64 (1978).